


 Cite this: *RSC Adv.*, 2024, **14**, 10755

Photocatalyzed hydrodecarboxylation of fatty acids: a prospective method to produce drop-in biofuels†

Amanda M. de Azevedo, Jhudson G. L. de Araujo, Maria do S. B. da Silva, Aecia S. D. dos Anjos, Aruzza M. M. de Araújo, Elisama V. dos Santos, Carlos Alberto Martínez-Huitle, Amanda D. Gondim and Lívia N. Cavalcanti *^{*}

A direct and practical method for photocatalyzed hydrodecarboxylation of fatty acids is reported herein. The catalytic system consists of a commercially available acridinium salt as the photocatalyst and thiophenol as the Hydrogen Atom Transfer (HAT) co-catalyst. Results evidenced that C_{n-1} alkanes were obtained in yields up to 77%. Furthermore, the protocol was employed for a complex mixture of fatty acids bio-derived from a real sample of licuri oil to obtain hydrocarbons in the range of C_9 – C_{17} with high selectivity and excellent conversion (>90%). This work provides a powerful strategy for producing drop-in biofuels under mild conditions. Finally, an energetic assessment of our proposed protocol (~22.9 kW h) reveals the benefit of a sustainable production of renewable hydrocarbons.

Received 15th February 2024

Accepted 27th March 2024

DOI: 10.1039/d4ra01166j

rsc.li/rsc-advances

Introduction

The excessive use of fossil fuels, driven by the growing global energy demand, has significantly contributed to the increase in greenhouse gas emissions, mainly CO_2 , in the atmosphere. This scenario plays a crucial role in the increase of global warming and the occurrence of some climate changes.^{1–3} Specifically, the transportation sector still heavily relies on petroleum derivatives, being responsible for 23% of global CO_2 emissions related to energy in 2019.⁴ In this regard, the deployment of low-carbon fuels that support the decarbonization of this sector, to meet the climate mitigation goals established in the Paris Agreement of 2015, depends on the change of alternative fuels instead of petroleum-derived.^{5–7}

In this transition context, conventional biofuels, such as biodiesel, for instance, play a significant role.^{8,9} However, their oxygenated composition results in significant undesirable properties, such as low thermal and oxidative stability. These characteristics lead to compatibility issues in current engines, limiting their use to blending with fossil diesel.^{10–12} Therefore, the pursuit of oxygen-free fuels is currently desirable, such as drop-in biofuels, composed of a mixture of renewable hydrocarbons, which are fully compatible with the current vehicle infrastructure.^{13–16}

These fuels can be obtained by deoxygenation of vegetable oils and other biomass *via* thermochemical routes, such as

hydrotreatment and thermocatalytic pyrolysis. Despite the efficiency of these processes, the necessity for high temperatures (up to 500 °C), elevated hydrogen gas pressures (>10 bar), and the use of metallic catalysts represent considerable disadvantages of the procedures.^{17–23} Hence, there is a strong motivation to investigate efficient deoxygenation methods to circumvent these harsh conditions.

Among the approaches that use less severe operating conditions, photocatalytic processes have emerged as an alternative to traditional protocols.^{24–28} In this sense, photocatalysis has been demonstrating significant advancements in the synthesis of value-added chemical products.^{29–32} Specifically, it has increased the interest in investigating these processes aiming at deoxygenation reactions of carboxylic acids to generate alkanes, including instances involving bioderived fatty acids that produce hydrocarbons chemically identical to drop-in biofuels.

For instance, alkanes have been obtained with high yields and remarkable selectivity through the photocatalytic hydrodecarboxylation of fatty acids using Pt/TiO_2 and Ni/TiO_2 as photocatalysts under H_2 pressure and UV light irradiation.^{24,33} Although these systems are comparable in efficiency to conventional methods, the requirement of a H_2 atmosphere to promote rapid termination of alkyl radicals reduces the process's sustainability, as this gas is primarily derived from non-renewable sources.³⁴

To steer clear of using hydrogen gas and simultaneously prevent secondary reactions arising from the instability of the primary radicals formed, several protocols use more easy-to-handle hydrogen atom transfer (HAT) co-catalyst, like thiols and disulfides.^{26,35} In this context, Nicewicz and colleagues

Federal University of Rio Grande do Norte, Institute of Chemistry, 59072-970, Natal, RN, Brazil. E-mail: livia.cavalcanti@ufrn.br

† Electronic supplementary information (ESI) available. See DOI: <https://doi.org/10.1039/d4ra01166j>



reported a direct photocatalytic system using an acridinium salt as a photocatalyst (Mes-Acr-Ph), diphenyl disulfide as HAT co-catalyst, and *N,N*-diisopropylethylamine (DIPEA) for the hydrodecarboxylation of various aliphatic carboxylic acids into alkanes²⁷ in high yields. However, the reaction scope was limited to only one fatty acid (tridecanoic acid). It is also important to indicate that the yield of dodecane was increased up to 49%, after adjusting the optimized condition by increasing reaction time and co-catalyst stoichiometry. Additionally, the use of a very expensive solvent, trifluoroethanol (TFE), was required to guarantee the success of the reaction for transforming primary carboxylic acids (Scheme 1a).

Within this framework, Li²⁸ and colleagues recently adapted Nicewicz's method²⁷ developing a visible light photocatalyzed decarboxylation strategy to favor the fatty acids transformation to alkanes,²⁸ optimizing the reaction for bioderived fatty acids and avoiding the use of TFE as solvent. This system consisted of combining a methoxy-substituted acridinium compound as a photocatalyst (Mes-1,3,6,8-tetramethoxy-Acr-3'',5''-dimethoxy-Ph), 4',4'-dimethyl diphenyldisulfane as a HAT catalyst, and *n*-Bu₄OAc in EtOAc to provide the production of alkanes (C₉–C₁₇) in high yields. Nevertheless, the method also proved to be efficient in the hydrodecarboxylation of a mixture of tridecanoic acid and dodecanoic acid in a 1 : 1 molar ratio under standard conditions (Scheme 1b).

Although the protocols of Nicewicz and Li have demonstrated impressive outcomes, a method for the direct catalytic hydrodecarboxylation of fatty acids using a commercial acridinium salt remained undefined. Moreover, it is highly desirable to extend this transformation to more complex fatty acid mixtures to those previously examined to confirm the method's robustness and reliability.

Herein we describe a sustainable photocatalytic decarboxylation route for conversion of bio-derived fatty acids into alkanes (C₉–C₁₇) using a commercial acridinium salt (Mes-Acr-Me) as the photocatalyst, thiophenol as a HAT co-catalyst, and an inexpensive inorganic base (NaHCO₃) in toluene/H₂O (9 : 1) under blue LED irradiation (Scheme 1c).

To the best of our knowledge and based on the existing literature, this is the first photocatalytic hydrodecarboxylation method for bio-derived fatty acids obtained from the hydrolysis of vegetable oils to produce aviation biofuel-range hydrocarbons using a commercially available acridinium salt as photocatalyst in a metal and hydrogen gas-free protocol. Also, this approach was electrically-economically evaluated to demonstrate the advantage of achieving sustainable production of renewable hydrocarbons.

Results and discussion

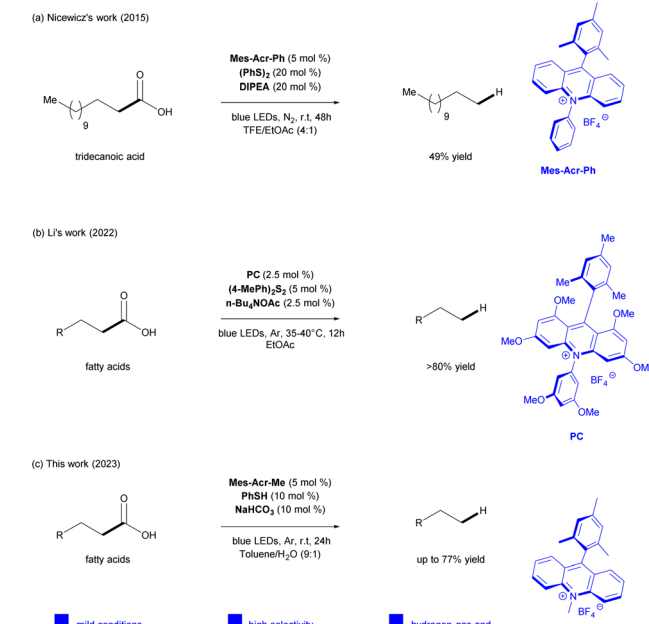
We began the optimization process with similar conditions to those previously reported by Nicewicz's lab and Li's group. Thus, using a commercially available acridinium salt (Mes-Acr-Me) as photocatalyst, thiophenol (PhSH) as HAT co-catalyst and *N,N*-diisopropylethylamine (DIPEA) in CHCl₂ under blue LED irradiation ($\lambda_{\text{max}} = \sim 450$ nm, 7 W) over 24 h at room temperature under N₂ atmosphere conditions. Lauric acid (**1a**) was chosen as a model substrate because it is the major component in some vegetable oils, such as licuri, babassu, and coconut, which are promising feedstocks to produce biofuels.^{36–39} Under these initial conditions, only a trace of *n*-undecane (**2a**) was assessed (Table 1, entry 1).

Subsequently, a solvent screening was performed (see ESI,† Section 5.1). The solvents were chosen based on the existing

Table 1 Optimization of reaction conditions^a

Entry	Deviation from above	Yield ^b (%)
1	None	<5
2	Toluene/H ₂ O (9 : 1) as solvent	44
3	10 mol% of DIPEA	59
4	5 mol% of thiophenol	40
5	20 mol% of thiophenol	60
6	NaHCO ₃ instead of DIPEA	57
7	Two blue LEDs (~ 450 nm, 7 W)	61
8	No photocatalyst	0
9	No base	0
10	No thiophenol	11
11	Open atmosphere	34
12	Argon atmosphere	77
13	Oxygen atmosphere ^c	12

^a Reactions carried out on a 0.2 mmol scale in N₂-sparged solvents [0.1 M] at ambient temperature for 24 h. ^b Yields determined by GC-MS using hexadecane as internal standard. ^c The yield of oxygenated by-products was 60%.



Scheme 1 Pathways for hydrodecarboxylation of fatty acids.



literature.^{26–28,40} Reactions were carried out on a 0.2 mmol scale in N_2 -sparged solvents, considering a concentration of about 0.1 mol L⁻¹, at ambient temperature for 24 h, and the yield was determined from GC-MS data by using hexadecane as an internal standard. According to the data the mixture toluene/H₂O (9 : 1) was considered the ideal solvent system providing **2a** in 44% (Table 1, entry 2). The result agrees with the findings from Nicewicz's group²⁷ evidencing that the water–solvent proportion–system significantly improved the yield. This may be related to the increase of the equilibrium concentration of carboxylate compared to carboxylic acid, caused by the addition of a more polar solvent, such as water, which facilitates proton dissociation and promotes the stabilization of carboxylate ions through ion–dipole interaction.⁴¹

Next, the stoichiometry of the reagents was examined. Decreasing the load of Mes-Acr-Mes harms the reaction outcome (see ESI,† Section 5.2). As observed in Table 1 (entry 3), the yield of **2a** increased by reducing the base stoichiometry to 10 mol%. The thiophenol stoichiometry can be maintained at 10 mol%, which is considered the ideal conversion condition, because the product yield was not improved independently of a decrease/increase in the load of this reagent (Table 1, entries 4 and 5).

It is important to consider that the base plays a crucial role in the photocatalyzed transformations. In fact, it generates the carboxylate anion and drives the reaction, therefore, various organic and inorganic bases were tested (see ESI,† Section 5.4). Notably, to our delight, we managed to use NaHCO₃, a low-cost and readily accessible base without any losses in product formation (see Table 1, entry 6). As a subsequent step in the screening study, the influence of irradiation on the process was investigated (Table 1, entry 7). As can be observed in Table 1, the use of two LED lamps ($\lambda_{\text{max}} = \sim 450$ nm, 7 W) promotes an increase in the yield of product **2a** (entry 7). Finally, control

experiments show the importance of combining photocatalyst, base, and HAT cocatalyst to efficiently promote the reaction (Table 1, entries 8–10).

Another factor that has been identified as a key operating condition, is the reaction atmosphere. The presence of oxygen in the reaction medium allowed side oxidation reactions that limited the efficiency of the photocatalyzed hydrodecarboxylation of fatty acids.⁴² Therefore, different atmosphere conditions were also examined. On the one hand, a decrease in the product's yield of **2a** is achieved (Table 1, entry 11) when open atmosphere conditions were used. On the other hand, the use of argon led to an increase in the yield of product **2a** (Table 1, entry 12). Thus, the optimization studies indicated that the hydrodecarboxylation of lauric acid (**1a**) using Mes-Acr-Me (5 mol%), thiophenol (10 mol%), and NaHCO₃ (10 mol%) under two blue LEDs irradiation ($\lambda_{\text{max}} = \sim 450$ nm, 7 W) over 24 h at room temperature under argon atmosphere are the most suitable conditions to promote the significant yield achievement of undecane (**2a**) at 77% and a conversion of lauric acid (**1a**) at 82%. During the optimization process, we observed the formation of oxygenated by-products in trace amounts. Because of that, we conducted a control experiment in an oxygen atmosphere (Table 1, entry 13) to elucidate the formation of these derivatives, which increased in this atmosphere. The presence of oxygen in decarboxylation has been mentioned in previous studies.^{42–44} Hence, it can be inferred that the composition of the reaction atmosphere impacts the preference for the formation of these products.

Furthermore, we calculated the turnover number (TON) and the turnover frequency (TOF) to evaluate our catalytic system's effectiveness (refer to ESI,† Section 6). In optimized conditions, the TON was 15.4 and the TOF was 1.78×10^{-4} Hz. These data are crucial for understanding our system's catalytic activity and for comparing catalysts in similar studies. Comparison with

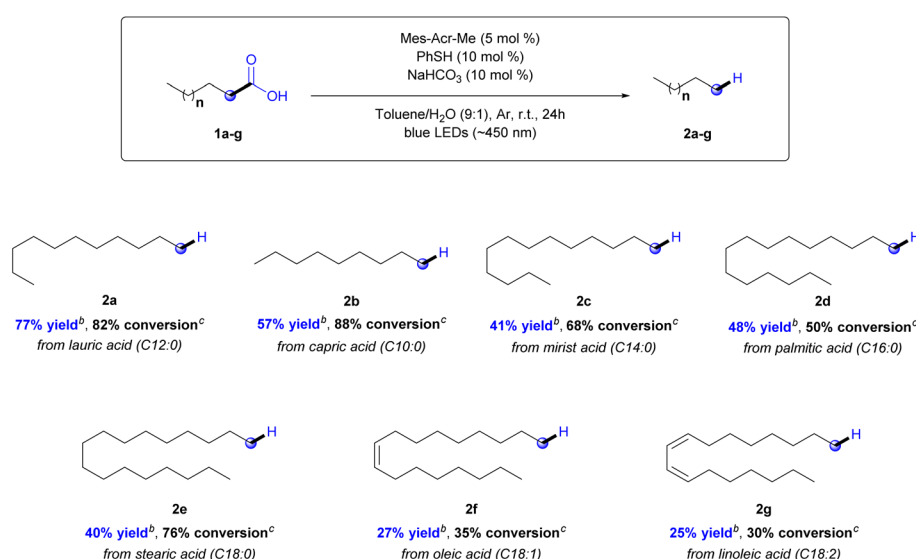


Chart 1 Photocatalytic hydrodecarboxylation reaction scope.^a Reactions conditions: **1a–g** (0.2 mmol), Mes-Acr-Me (5 mol%), PhSH (10 mol%), NaHCO₃ (10 mol%), toluene/H₂O (9 : 1, 2 mL), 7 W blue LEDs (~ 450 nm), argon atmosphere, rt, 24 h.^b Yields were determined by GC-FID using a calibration curve. Conversions were determined by GC-FID using a calibration curve.



Table 2 Fatty acids composition of licuri oil

Fatty acids	Experimental results ^a [%]	Literature ⁴⁷ [%]
Caprylic acid (C8 : 0)	5.0	9.0
Capric acid (C10 : 0)	6.0	6.0
Lauric acid (C12 : 0)	49.0	42.0
Myristic acid (C14 : 0)	17.0	16.0
Palmitic acid (C16 : 0)	8.0	8.0
Stearic acid (C18 : 0)	2.0	4.0
Oleic acid (C18 : 1)	13.0	12.0
Linoleic acid (C18 : 2)	—	3.0

^a Values determined by GC-MS using relative distribution.

literature values for the same photocatalyst revealed a significant TON variation (typically 2 to 8), depending on the photocatalyst's stoichiometry.^{44,45} Our protocol demonstrated notably higher efficiency, indicating greater catalyst effectiveness and promising practical application potential.

With these optimized conditions, the next step was to study the scope of the reaction (Chart 1). Fatty acids with different carbon chains were evaluated (C₁₀–C₁₈). The yields were determined using a GC-FID calibration curve (see ESI,† Section 4). According to the results, the developed protocol demonstrated high selectivity to produce hydrocarbons (2a–g) in moderate yields, ranging from 77 to 25%, and conversion ranging from 88 to 30%, depending on the starting material (Chart 1).

Finally, we evaluated the robustness of the developed method in the application of a complex mixture of bio-derived fatty acids obtained by hydrolysis of vegetable oil (see ESI,† Section 7). The chosen biomass was licuri oil because it contains fatty acids with carbon chain lengths ranging from C₈ to C₁₈ (Table 2), which had been previously identified as a promising feedstock to produce sustainable biojet fuel through catalytic deoxygenation processes.⁴⁶ Additionally, it can be used in the production of green diesel, providing n-alkanes with carbon chains ranging from C₁₄ to C₁₇.

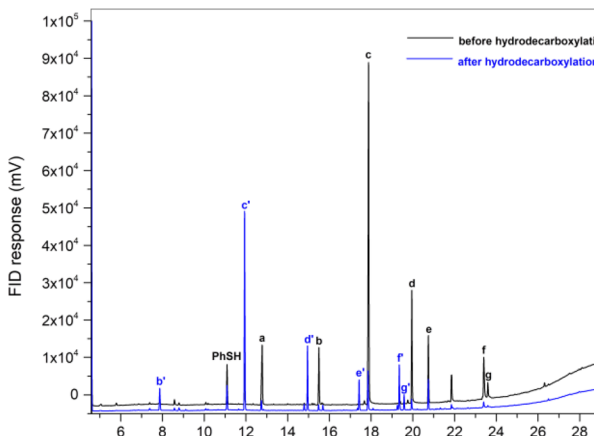


Fig. 1 Chromatograms of bio-derived fatty acids from licuri oil before (black) and after photocatalytic hydrodecarboxylation (blue). (a) Caprylic acid, (b) capric acid, (c) lauric acid, (d) myristic acid, (e) palmitic acid, (f) oleic acid, (g) stearic acid, (b') n-nonane, (c') n-undecane, (d') n-tridecane, (e') n-pentadecane, (f') heptadec-8-ene, (g') n-heptadecane, (PhSH) thiophenol.

Encouraging results were found when a complex mixture of fatty acids of licuri oil was submitted to the optimized protocol conditions, resulting in a variety of n-alkanes in the range of C₉–C₁₇, with remarkable selectivity and a substrate conversion of over 90%. All n-alkanes were detected by GC-FID (Fig. 1), except n-heptane, which was not detected using the analysis method employed. The products obtained demonstrated that this photocatalytic method is an elegant way to produce hydrocarbons compatible with drop-in biofuels *via* vegetable oil deoxygenation.

Given that this study's approach aims at producing sustainable biofuels, it is crucial to continuously enhance the process by reducing energy consumption and carbon emissions. As far as we know, previously reported works do not calculate the energy expenditures associated with their photocatalysis methodologies in organic synthesis. However, electrical energy consumption (EEC), referred to as electrical energy per order (E_{EO}) in cases of low pollutant concentrations, is the major figure-of-merit for comparing operational costs in advanced oxidative processes, such as heterogeneous photocatalysis.^{48,49} According to IUPAC, E_{EO} is the number of kilowatt hour of electrical energy required to reduce the concentration of a pollutant by 1 order of magnitude (90%) in a unit volume of contaminated water.^{50–54} In this context, an adjustment was made to this concept to assess the process's electrical energy consumption by calculating the kilowatt hour (kW h) needed to carry out a reaction according to the methodology presented in this study, as per the equation below.

$$E(\text{kW h}) = \frac{P(\text{W}) \times t(\text{h})}{1000} \quad (1)$$

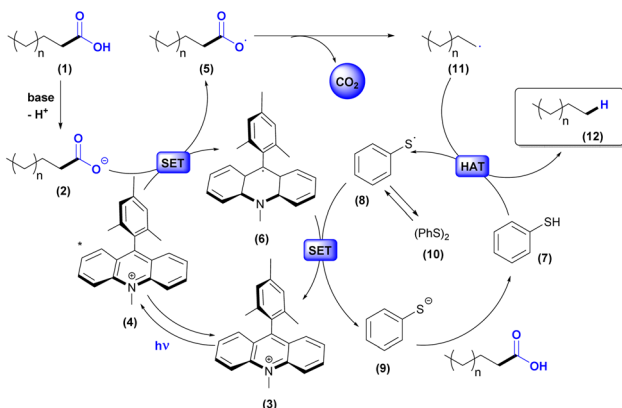
where E is the electrical energy consumption, P is the equipment power and t is the usage time. For this, the parameters of eqn (1) were considered for the three electrical devices involved: the two LED lamps, the magnetic stirrer, and the fan. As shown in Table 3, it can be observed that the energy consumption was 22.9 kW h for one reaction. As organic synthesis methodologies do not conduct this kind of techno-economic study, it was not possible to compare it with other photocatalytic methods published in the existing literature. However, this simple techno-energetic requirement assessment shows that such selectivity allows to evaluate the photocatalytic hydrodecarboxylation protocol to be economically profitable and generate drop-in biofuels at a cost that is competitive with other methodologies.

Table 3 Energy consumption of the electrical devices used in the photocatalytic process

Electrical appliance	Equipment power (W)	Electrical energy consumption ^a (kW h)
Two LED lamps	7 (each lamp)	0.336
Magnetic stirrer	800	19.2
Fan	140	3.36
Total	954	22.9

^a Calculated consumption for 24 hours of use (time for one reaction).





Scheme 2 Proposed mechanism for hydrodecarboxylation.

Based on previous works presented in Scheme 1, we propose the mechanism illustrated in Scheme 2. Firstly, the carboxylic acid (1) is deprotonated to afford the carboxylate anion (2). Meanwhile, Mes-Acr-Me⁺ (3) is excited under visible light irradiation and converted to the long-lived electron transfer state (4). Next, a single electron transfer occurs between the carboxylate anion (2) and the excited photocatalyst (4) to generate the acridine radical (6) and the carboxyl radical (5). Subsequently, decarboxylation of the carboxyl radical affords the carbon-centered alkyl radical (11), which, after undergoing atomic hydrogen transfer with thiophenol (7), forms the alkane (12) and the thiyl radical (8). The latter acts as a one-electron oxidant for the acridine radical (6) in the other concomitant catalytic cycle and, therefore, regenerates the photocatalyst in its ground state (3) and produces the thiolate (9). Protonation of PhS⁻ (10) with H⁺ from (1) can regenerate the thiophenol (7). Phenyl disulfide (10) can be formed in the reaction by radical S-S coupling and exists in equilibrium with (8).^{40,55} From this, the synergy between the catalytic cycles indicates the sustainability of the process by allowing the renewal of species in the medium through redox processes.

Conclusions

In summary, we have described a direct photocatalytic protocol using a commercial acridinium salt for hydrodecarboxylation of a variety of fatty acids to afford *n*-alkanes. We also extended this method to bioderived fatty acids from licuri oil and concluded that it provides an efficient route for hydrocarbon production, especially in the jet fuel range. According to the results, fatty acids were converted into alkanes with high selectivity and moderate yields. Scope investigation revealed that chain length and unsaturated substrates led to a decrease in yield. The method is well-established at room temperature and pressure, without the need for hydrogen gas or metallic catalysts, which are milder conditions compared to conventionally used thermocatalytic techniques. The estimation of electrical requirements for the system showed a total expenditure of 22.9 kW h per reaction, which could be significantly enhanced when the photocatalyzed hydrodecarboxylation of fatty acids protocol is

coupled with renewable energies,⁵⁶ revealing the benefit of zero-carbon emissions and positive carbon credits.

Author contributions

Azevedo AM: methodology, formal analysis, investigation, writing – review & editing, Araujo JGL; Silva MSB: methodology and formal analysis, Anjos ASD; Araújo AMM: formal analysis; dos Santos EV; Martínez-Huitl CA: writing – review & editing, Gondim AD: conceptualization, supervision, Cavalcanti LN: conceptualization, validation, review & editing, supervision.

Conflicts of interest

There are no conflicts to declare.

Acknowledgements

This work was generously supported by Programa de Formação de Recursos Humanos of ANP (PRH 37/ANP) through Programa de Pós-graduação em Química at UFRN (PPGQ-UFRN). The authors would like to thank the Analytical Center at Institute of Chemistry (IQ-UFRN) and Núcleo de Processamento Primário Reuso de Água Produzida e Resíduos of UFRN (Nupprar/UFRN) for providing GC-MS and GC-FID analysis.

Notes and references

- 1 A. C. Jones, M. K. Hawcroft, J. M. Haywood, A. Jones, X. Guo and J. C. Moore, *Earth's Future*, 2018, **6**, 230–251.
- 2 IPCC, in *Global Warming of 1.5 °C*, Cambridge University Press, 2022, pp. 175–312.
- 3 L. R. Boysen, W. Lucht, D. Gerten, V. Heck, T. M. Lenton and H. J. Schellnhuber, *Earth's Future*, 2017, **5**, 463–474.
- 4 I. Energy Agency, *Global Energy Review*, 2020.
- 5 M. Klöwer, M. R. Allen, D. S. Lee, S. R. Proud, L. Gallagher and A. Skowron, *Environ. Res. Lett.*, 2021, **16**, 104027.
- 6 S. Gota, C. Huizenga, K. Peet, N. Medimorec and S. Bakker, *Energy Effic.*, 2019, **12**, 363–386.
- 7 P. Vozka and G. Kilaz, *Fuel*, 2020, 268.
- 8 N. S. Mat Aron, K. S. Khoo, K. W. Chew, P. L. Show, W. H. Chen and T. H. P. Nguyen, *Int. J. Energy Res.*, 2020, **44**, 9266–9282.
- 9 H. Wang, B. Yang, Q. Zhang and W. Zhu, *Renewable Sustainable Energy Rev.*, 2020, **120**, 109612.
- 10 K. B. Baharudin, N. Abdullah, Y. H. Taufiq-Yap and D. Derawi, *J. Cleaner Prod.*, 2020, **274**, 122850.
- 11 M. A. Díaz-Pérez and J. C. Serrano-Ruiz, *Molecules*, 2020, **25**.
- 12 Y. K. Oh, K. R. Hwang, C. Kim, J. R. Kim and J. S. Lee, *Bioresour. Technol.*, 2018, **257**, 320–333.
- 13 M. Y. Kim, J. K. Kim, M. E. Lee, S. Lee and M. Choi, *ACS Catal.*, 2017, **7**, 6256–6267.
- 14 B. P. Pattanaik and R. D. Misra, *Renewable Sustainable Energy Rev.*, 2017, **73**, 545–557.
- 15 H. Kargbo, J. S. Harris and A. N. Phan, *Renewable Sustainable Energy Rev.*, 2021, **135**, 110168.



16 T. A. Palankoev, K. I. Dementiev and S. N. Khadzhiev, *Pet. Chem.*, 2019, **59**, 438–446.

17 L. C. T. Andrade, G. J. Muchave, S. T. A. Maciel, I. P. Da Silva, G. F. Da Silva, J. M. A. R. Almeida and D. A. G. Aranda, *Int. J. Chem. Eng.*, 2022, **2022**, 6402004.

18 A. Sonthalia and N. Kumar, *J. Energy Inst.*, 2019, **92**, 1–17.

19 K. Rambabu, G. Bharath, N. Sivarajasekar, S. Velu, P. N. Sudha, S. Wongsakulphasatch and F. Banat, *Fuel*, 2023, **331**, 125688.

20 P. Lahijani, M. Mohammadi, A. R. Mohamed, F. Ismail, K. T. Lee and G. Amini, *Energy Convers. Manage.*, 2022, **268**, 115956.

21 A. Miro de Medeiros, K. de Sousa Castro, M. L. Gundim de Macêdo, A. Mabel de Moraes Araújo, D. Ribeiro da Silva and A. D. Gondim, *RSC Adv.*, 2022, **12**, 10163–10176.

22 Nishu, R. Liu, M. M. Rahman, M. Sarker, M. Chai, C. Li and J. Cai, *Fuel Process. Technol.*, 2020, **199**, 106301.

23 K. de Sousa Castro, L. Fernando de Medeiros Costa, V. J. Fernandes, R. de Oliveira Lima, A. Mabel de Moraes Araújo, M. C. Sousa de Sant'Anna, N. Albuquerque dos Santos and A. D. Gondim, *RSC Adv.*, 2020, **11**, 555–564.

24 Z. Huang, Z. Zhao, C. Zhang, J. Lu, H. Liu, N. Luo, J. Zhang and F. Wang, *Nat. Catal.*, 2020, **3**, 170–178.

25 N. Li, Y. Ning, X. Wu, J. Xie, W. Li and C. Zhu, *Chem. Sci.*, 2021, **12**, 5505–5510.

26 J. G. Leandro de Araujo, M. do S. Bezerra da Silva, J. C. Celeste Viana Bento, A. Medeiros de Azevêdo, A. M. de Moraes Araújo, A. S. Dantas dos Anjos, C. A. Martinez Huitle, E. Vieira Dos Santos, A. D. Gondim and L. Cavalcanti, *Chem.-Eur. J.*, 2023, **29**, e2023023.

27 J. D. Griffin, M. A. Zeller and D. A. Nicewicz, *J. Am. Chem. Soc.*, 2015, **137**, 11340–11348.

28 Y. L. Sun, F. F. Tan, R. G. Hu, C. H. Hu and Y. Li, *Chin. J. Chem.*, 2022, **40**, 1903–1908.

29 F. Ma, Q. Tang, S. Xi, G. Li, T. Chen, X. Ling, Y. Lyu, Y. Liu, X. Zhao, Y. Zhou and J. Wang, *Chin. J. Catal.*, 2023, **48**, 137–149.

30 A. Raja, N. Son, M. Swaminathan and M. Kang, *Chem. Eng. J.*, 2023, **468**, 143740.

31 Y. Zhu, R. Tan, C. Yang, B. Zhang, K. Deng, D. Tang and D. Ding, *Mol. Catal.*, 2024, **554**, 113818.

32 A. Gottuso, C. De Pasquale, S. Livraghi, L. Palmisano, S. Diré, R. Ceccato and F. Parrino, *Mol. Catal.*, 2023, **550**, 113607.

33 X. Du, Y. Peng, J. Albero, D. Li, C. Hu and H. García, *ChemSusChem*, 2022, **15**, e2021021.

34 S. M. Jokar, A. Farokhnia, M. Tavakolian, M. Pejman, P. Parvasi, J. Javanmardi, F. Zare, M. C. Gonçalves and A. Basile, *Int. J. Hydrogen Energy*, 2023, **48**, 6451–6476.

35 M. O. Zubkov, M. D. Kosobokov, V. V. Levin and A. D. Dilman, *Org. Lett.*, 2022, **24**, 2354–2358.

36 C. L. Nicolau, A. N. V. Klein, C. A. A. Silva, A. R. Fiorucci, J. M. Stropa, E. O. Santos, K. C. S. Borges, R. C. L. Da Silva, L. C. S. De Oliveira, E. L. Simionatto, D. R. Scharf and E. Simionatto, *J. Braz. Chem. Soc.*, 2018, **29**, 1672–1679.

37 Y. Sugami, E. Minami and S. Saka, *Fuel*, 2017, **197**, 272–276.

38 M. Al-Muttaqii, F. Kurniawansyah, D. H. Prajitno and A. Roesyadi, *Indones. J. Chem.*, 2019, **19**, 319–327.

39 P. H. M. Araújo, A. S. Maia, A. M. T. M. Cordeiro, A. D. Gondim and N. A. Santos, *ACS Omega*, 2019, **4**, 15849–15855.

40 C. Cassani, G. Bergonzini and C. J. Wallentin, *Org. Lett.*, 2014, **16**, 4228–4231.

41 Y. E. Zevatskii, D. V. Samoilov and N. O. McHedlov-Petrosyan, *Russ. J. Gen. Chem.*, 2009, **79**, 1859–1889.

42 Z. Bazyar and M. Hosseini-Sarvari, *J. Org. Chem.*, 2019, **84**, 13503–13515.

43 M. Uygur, J. H. Kuhlmann, M. C. Pérez-Aguilar, D. G. Piekarski and O. García Mancheño, *Green Chem.*, 2021, **23**, 3392–3399.

44 Q. Chen, Y. Wang and G. Luo, *Chem. Eng. J.*, 2023, **461**, 141767.

45 K. Ohkubo, A. Fujimoto and S. Fukuzumi, *Chem. Commun.*, 2011, **47**, 8515–8517.

46 J. L. F. Oliveira, L. M. B. Batista, N. Albuquerque dos Santos, A. M. M. Araújo, V. J. Fernandes, A. S. Araújo, A. P. M. Alves and A. D. Gondim, *Renewable Energy*, 2021, **168**, 1377–1387.

47 K. Teixeira da Silva de La Salles, S. M. P. Meneghetti, W. Ferreira de La Salles, M. R. Meneghetti, I. C. F. dos Santos, J. P. V. da Silva, S. H. V. de Carvalho and J. I. Soletti, *Ind. Crops Prod.*, 2010, **32**, 518–521.

48 S. O. Ganiyu, M. Zhou and C. A. Martínez-Huitle, *Appl. Catal. B*, 2018, **235**, 103–129.

49 C. A. Martínez-Huitle, M. A. Rodrigo, I. Sirés and O. Scialdone, *Appl. Catal. B*, 2023, **328**, 122430.

50 K. P. Sundar and S. Kanmani, *Chem. Eng. Res. Des.*, 2020, **154**, 135–150.

51 H. Eskandarloo, A. Badiei, M. A. Behnajady and G. M. Ziarani, *RSC Adv.*, 2014, **4**, 28587–28596.

52 V. Vaiano, O. Sacco and D. Sannino, *J. Cleaner Prod.*, 2019, **210**, 1015–1021.

53 D. B. Miklos, C. Remy, M. Jekel, K. G. Linden, J. E. Drewes and U. Hübner, *Water Res.*, 2018, **139**, 118–131.

54 N. Modirshahla, M. A. Behnajady, R. Rahbarfam and A. Hassani, *Clean*, 2012, **40**, 298–302.

55 N. A. Romero and D. A. Nicewicz, *J. Am. Chem. Soc.*, 2014, **136**, 17024–17035.

56 S. O. Ganiyu, C. A. Martínez-Huitle and M. A. Rodrigo, *Appl. Catal. B*, 2020, **270**, 118857.

